Hospital of Stomatology[1], Guanghua School of Stomatology, Sun Yat-sen University; Guangdong Provincial Key Laboratory of Stomatology[2]; Guangdong Provincial Key Laboratory of New Drug Screenin[3], School of Pharmaceutical Sciences, Southern Medical University; Department of Oral and Maxillofacial Surgery[4], Nanfang Hospital, Southern Medical University, Guangzhou, China

Non-classical platinum-based compound 56MESS, with preferential cytotoxic effect on oral cancer cells by downregulating FACL4 expression

Lejing Miao[1,2], Pei Yu[1,2], Jing Huang[1,2], Zehang Zhuang[1,2], Zhiqiang Yu[3], Xiqiang Liu[1,2,4,*]

Received April 21, 2020, accepted May 22, 2020

**Corresponding author: Xiqiang Liu, Hospital of Stomatology, Guangdong Provincial Key Laboratory of Stomatology, Sun Yat-sen University, No. 56, Lingyuan West Road, Guangzhou 510055, China*
liuxiq@mail.sysu.edu.cn

Pharmazie 75: 494-499 (2020) *doi: 10.1691/ph.2020.0481*

Platinum (Pt)-based drugs are routinely used to treat oral cancer (OC), but occurrence of therapeutic resistance remains a formidable challenge in cancer treatment. We sought to explore the cytotoxicity of non-classical Pt-based compounds, and compared the efficacy and anticancer activity of 56MESS with cisplatin in OC. Drug sensitivity of seven non-classical Pt-based compounds as well as cisplatin were determined by CCK-8 assay. Comparison of cytotoxic effects between 56MESS, phenanthriplatin and cisplatin was performed on six different OC cell lines. The anticancer effects of 56MESS was further measured both *in vitro* and *in vivo*. Additionally, the biological role of FACL4 and its relationship with 56MESS-induced growth inhibition were investigated. Two out of seven Pt-based compounds displayed a significant cytotoxic effect. 56MESS was chosen as the most potent compound due to its highly selective cytotoxic activity. 56MESS particularly caused G2/M phase arrest, while failed to induce apoptosis. *In vivo*, 56MESS had a higher cytotoxic capacity than cisplatin. Overexpression of FACL4 rescued 56MESS-induced growth inhibition in OC cells. Overall, 56MESS is a highly selective and potent chemotherapeutic drug superior to cisplatin, and thus may be considered as a promising anticancer agent.

1. Introduction

Oral cancer (OC) is a prevalent malignancy worldwide. According to the 2020 American cancer statistics, the incidence of OC ranks the eighth among malignancies in American male (Siegel et al. 2020). For advanced stage of OC, especially with metastasized lesions, Pt-based chemotherapy is a preferred option. Cisplatin is extensively used to treat many cancers (Dasari and Tchounwou 2014), but therapeutic resistance and its high toxicity remains an insurmountable challenge (Yu et al. 2010; Gonzales-Vitale, et al. 1997). Hence, efforts to explore novel alternatives with comparable or stronger anticancer efficacy and lower toxicity are urgently needed.

Over the past decades, only two platinum agents, i.e., carboplatin and oxaliplatin, have been brought to the market. Fortunately, the introduction inspired considerable efforts to further explore potentially effective platinum (Pt)-based agents. Among them, picoplatin, a third-generation bivalent Pt drug, can effectively overcome cisplatin and carboplatin resistance in small cell lung cancer cells (Tang et al. 2011). Picoplatin also demonstrated clinical efficacy in patients with Pt-refractory/-resistant lung cancers (Eckardt et al. 2009). Monofunctional Pt compounds, such as phenanthriplatin and pyriplatin can affect cellular DNA repair by forming DNA adducts, and exerted apparent anticancer effects on colon and breast cancers (Zhu et al. 2012; Gregory et al. 2014; Park et al. 2012). Multinuclear Pts, including BRR3005 and BRR3571 have also shown potential therapeutic effects on glioma and leukemia (Chopard et al. 2008). Moreover, a new family of non-classical Pt-based drugs, including Pt-Acrmatu and 56MESS, are more toxic to a variety of cancer cell lines than cisplatin (Suryadi and Bierbach 2012; Wang et al. 2012).

Here, we first evaluated the drug sensitivity of seven non-classical Pt-based compounds in OC cells (Fig. 1). The most potent compound 56MESS was then compared with cisplatin in terms of selective cytotoxic effects both *in vitro* and *in vivo*. We also evaluated the impact of FACL4 overexpression on 56MESS-mediated anticancer activity.

2. Investigations and results

2.1. Screening of the most potent Pt-based compounds

In order to select the most potent compound, we evaluated drug sensitivity of cisplatin and the seven Pt-based compounds in SCC15 and SCC25 cancer cells (Table 1). As shown, both

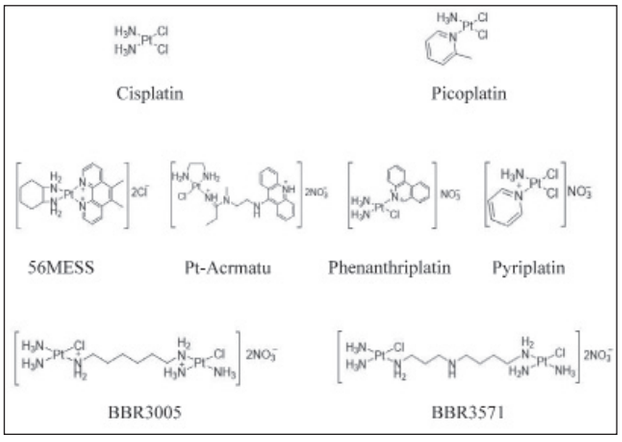

Fig. 1: Chemical structures of cisplatin and 7 non-classical platinum-based compounds.

phenanthriplatin and 56MESS had a higher cytotoxic effect than cisplatin. We further compared the difference of cytotoxicity between cisplatin, phenanthriplatin and 56MESS in an expanded OC cell panel (Table 2). Strikingly, 56MESS showed 33-91 times higher activity than cisplatin. Next, we assessed the toxic impact of the two compounds on human normal oral epithelial cells (hNOECs). Since neither phenanthriplatin nor 56MESS could kill 50% of hNOECs, it was impossible to determine IC_{50} values (data not shown). Therefore, 56MESS has a highly selective cytotoxic activity and was regarded as the most potent compound.

Table 1: IC_{50} (μM) values of 7 platinum-based compounds in oral cancer cell lines

Compound	IC_{50} [a]	
	SCC15	SCC25
56MESS	0. 064	0. 051
Phenanthriplatin	0. 367	0. 723
Cisplatin	4. 297	4. 654
Pt-Acrmatu	9. 201	8. 735
Pyriplatin	23. 697	26. 191
BBR3005	48. 421	5. 912
BBR3571	42. 837	6. 127
Picoplatin	46. 261	45. 013

[a] IC_{50} values are presented as mean from three repeating experiments.

Table 2: IC_{50} (μM) values of 56MESS, phenanthriplatin and cisplatin in 6 oral cancer cell lines

Cell line	IC_{50} [a]			Relative IC_{50} ratio [b]	
	Cisplatin	56MESS	Phen	56MESS	Phen
UM1	2. 371	0. 038	0. 264	62. 395	8. 981
HSC3	2. 373	0. 065	0. 371	36. 508	6. 396
CAL27	3. 222	0. 098	0. 456	32. 876	7. 066
SCC15	4. 297	0. 064	0. 367	67. 145	11. 708
CAL33	4. 362	0. 062	0. 467	70. 355	9. 341
SCC25	4. 654	0. 051	0. 723	91. 255	6. 437

[a] IC_{50} values are presented as mean from three repeating experiments. [b] Relative IC_{50} ratio equals to IC_{50} of cisplatin divided by IC_{50} of 56MESS or IC_{50} of phenanthriplatin. Phen: phenanthriplatin

2.2. *56MESS inhibits cell growth in vitro*

We performed EdU staining and colony formation assay to evaluate the ability of tumor cells growth *in vitro*. Our results showed that 56MESS significantly inhibited cell proliferation ($P < 0.01$, Fig. 2A, 2B). Of note, with only 1% concentration of cisplatin, comparable inhibition effects were observed in 56MESS-treated cells. Consistently, 56MESS significantly reduced colony formation of CAL33 and SCC25 cells in much lower concentration ($P < 0.01$, Fig. 2C, 2D). We further examined the impact of 56MESS on cell cycle. Although 56MESS and cisplatin caused G2/M phase arrest, less effect was observed in the 56MESS-treated cancer cells ($P < 0.05$ or $P < 0.01$, Fig. 3A).

2.3. *56MESS does not induce apoptosis*

Consistent with previous studies (Wang et al. 2000), our flow cytometric analyses confirmed the cisplatin-induced cell apoptosis. Unexpectedly, we failed to observe apoptosis in 56MESS-treated cancer cells ($P < 0.01$, Fig. 3B). Additionally, we performed a JC1 mitochondrial membrane potential (MMP) analysis. No change of MMP was observed after 56MESS treatment, in comparison significant decrease was detected after cisplatin treatment (Fig. S1). These results identified that 56MESS does not induce apoptosis.

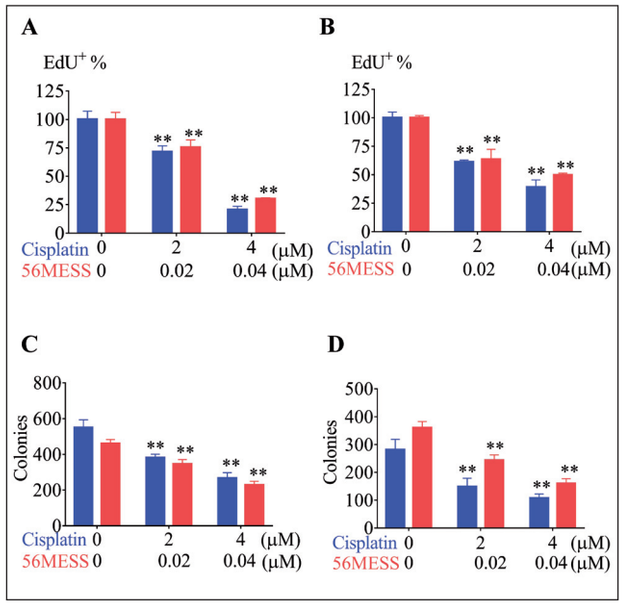

Fig. 2: 56MESS Inhibits oral cancer cell growth *in vitro*. CAL33 and SCC25 cells are treated with cisplatin and 56MESS with indicated concentration or negative control (DMSO). A, B. EdU staining analysis. The data are standardized against each cell line control and are presented as relative percent of the EdU-positive cells. C, D. colony formation assay performed after 10 days of treatment. The data are representative of 3 independent experiments. $*P < 0.05$, $**P < 0.01$.

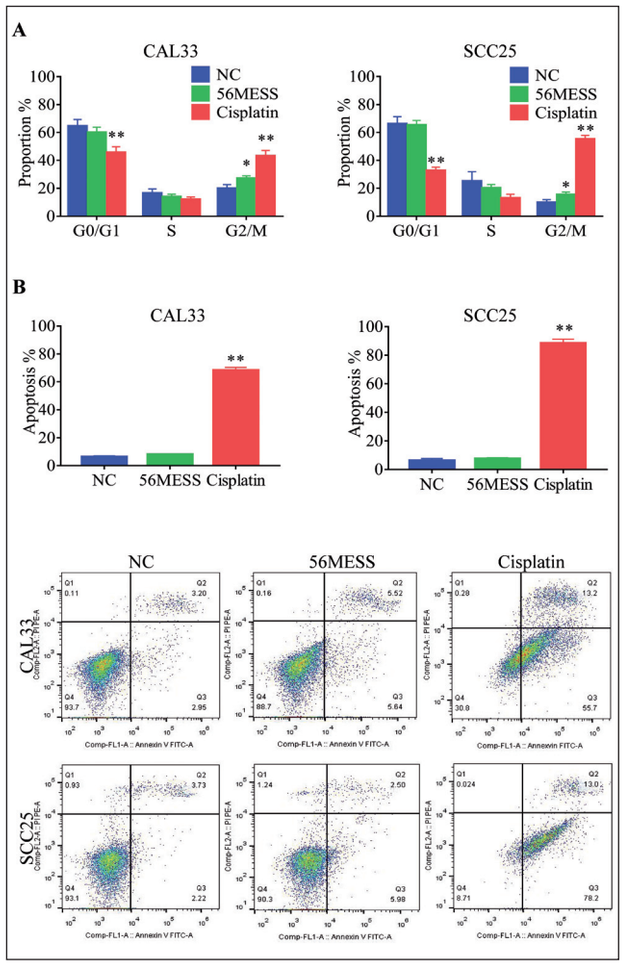

Fig. 3: 56MESS causes G2/M cell cycle arrest but fail to induce apoptosis. A. cell cycle analysis. B. cell apoptotic level measured by flow cytometric analysis. CAL33 and SCC25 cells are treated with 56MESS and cisplatin at their IC_{50} concentrations or DMSO (NC) for 48h. The data are representative of 3 independent experiments. NC: negative control (DMSO treatment). $*P < 0.05$, $**P < 0.01$.

2.4. 56MESS inhibits tumor growth in vivo

We first established an OC xenograft model on BALB/c nude mice, followed by repeated treatment as described in the Experimental section. Tumor volume and body weight of nude mice were measured regularly. Compared with the cisplatin-treated mice, 56MESS-treated ones had a much slower tumor growth ($P < 0.05$ or $P < 0.01$, Fig. 4A). Accordingly, the tumor weight of 56MESS-treated mice was significantly lower than that of cisplatin-treated ones ($P < 0.01$, Fig. 4B). We also observed more weight lost in the 56MESS-treated mice than that of cisplatin-treated ones ($P < 0.05$ or $P < 0.01$, Fig. 4C). Immunostaining showed that positive expression level of Ki67 significantly decreased in xenografts of 56MESS-treated mice, in comparison of that of cisplatin-treated and the control ones (Fig. S2). We further biopsied the mice kidney and found comparable microstructure changes in both 56MESS-treated mice and cisplatin-treated ones (Fig. S2). All together, these data showed that 56MESS had a potent anticancer effect *in vivo*.

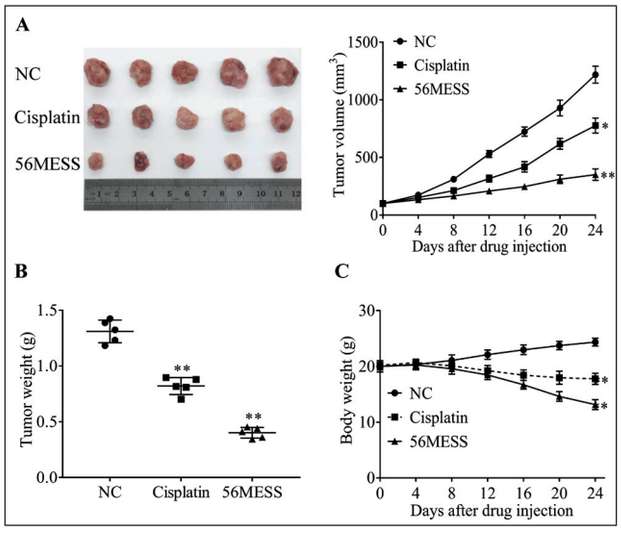

Fig. 4: *In vivo* anticancer activity of 56MESS in SCC25 xenograft model. The mice are tail vein injected with cisplatin (4 mg/kg), 56MESS (4 mg/kg), or DMSO. A. *Right*, photographs of the harvested tumors. *Left*, tumor growth curve. B. Tumor weight is measured at 24 days after the first treatment. C. Body weight curve. The body weight of mice is monitored every 4 days. $*P < 0.05$, $**P < 0.01$.

2.5. 56MESS downregulates FACL4 expression and FACL4 rescues 56MESS-induced growth inhibition

Deregulated lipid synthesis and uptake are contributing to fuel cancer cell proliferation. Here, we focus on action and contribution of FACL4, a fatty acid ligase to the 56MESS-mediated phenotype in OC. For this aim, we adopted UALCAN (http://ualcan.path.uab.edu) (Chandrashekar et al. 2017) to analyze the FACL4 mRNA expression of 520 head and neck cancers in the TCGA database. The mRNA level of FACL4 in cancers was upregulated ($P < 0.01$, Fig. 4A). To explore the possible relationship between FACL4 and 56MESS, OC cells were treated with 56MESS. As shown, the level of FACL4 mRNA and protein was reduced after 56MESS treatment ($P < 0.01$, Fig. 4B-4D). Consistently, the expression of FACL4 in xenografts of the 56MESS-treated mice was significantly reduced (Fig. 4E).

We then constructed a FACL4-overexpression plasmid and transiently transfected into cancer cells. The relative expression level of FACL4 mRNA and protein is normalized against each cell line control ($P < 0.01$, Fig. S3). As expected, overexpression of FACL4 significantly fueled tumor cell growth ($P < 0.01$, Fig. 4F). For determining whether 56MESS-induced growth inhibition is regulated by FACL4 expression, we further performed the rescue experiments. Strikingly, overexpression of FACL4 counteracted 56MESS-induced growth inhibition in CAL33 and SCC25 cells ($P < 0.01$, Fig. 4F).

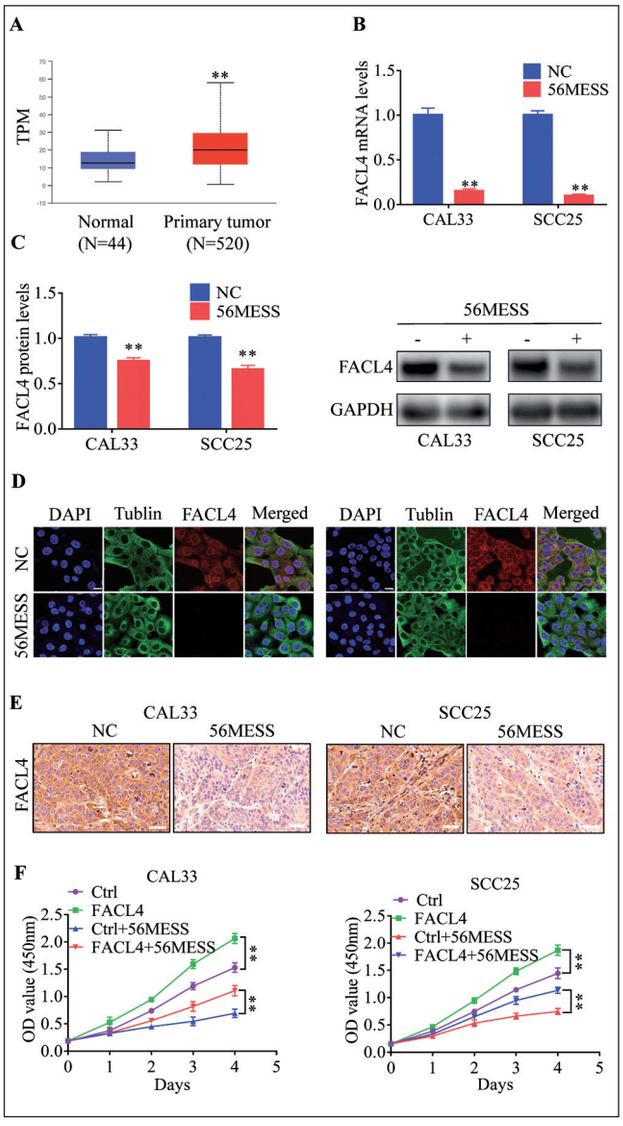

Fig. 5: FACL4 counteract 56MESS-induced growth inhibition. A. Boxplot shows the relative level of FACL4 mRNA in head and neck cancers compared with non-tumor tissues. UALCAN, an interactive web portal (http://ualcan.path.uab.edu) is performed to analyze the data extracted from the TCGA database. The mRNA level of FACL4 is normalized to a transcript per million readings (TPM). B, C. The level of FACL4 mRNA and protein after treated with 56MESS for 48h. D. Immunofluorescence staining of FACL4 in the 56MESS-treated or control (NC) cells. E. Immunostaining of FACL4 protein in xenografts of 56MESS-treated or control (DMSO-treated) mice. Scale bar: 100 μM. $*P < 0.05$, $**P < 0.01$. F. Overexpression of FACL4 rescued 56MESS-mediated cell growth inhibition. CAL33 and SCC25 cells are transiently transfected with FACL4-overexpression plasmid or control plasmid (NC), and then treated with 56MESS or DMSO for 48h. Cell viability is measured by CCK-8 assay and cell growth curves are depicted. $*P < 0.05$.

3. Discussion

In this study, we first screened the cytotoxic activity of seven Pt-based compounds in OC cells. These compounds can be arbitrarily classified into four categories, including bivalent (picoplatin), monofunctional (phenanthriplatin, pyriplatin), multinuclear (BRR3005, BRR3571) and metallointercalator (Pt-Acrmatu, 56MESS) compounds. The potency of phenanthriplatin and 56MESS was much higher than that of cisplatin in the tested cells. We then compared the spectrum of cytotoxic activity of phenanthriplatin, 56MESS and cisplatin in an extended OC cell line panel. Phenanthriplatin and 56MESS was 6-12 and 33-91 times more active than cisplatin, respectively.

Phenanthriplatin shows a spectrum of activity different from that of traditional platinum drugs (Monroe et al. 2018). Inhibition of RNA polymerases and DNA replication by phenanthriplatin lesions has been implicated in its mechanism of action (Gregory et al. 2014; Johnstone et al. 2014). The complex 56MESS is more active than the other platinum compounds tested so far (Krause-Heuer et al. 2009), which is consistent with our findings. Notably, 56MESS has found to be 163 times more active than cisplatin in a cisplatin-resistant mouse leukemia cell line (Wang et al. 2012). These results suggest that 56MESS is a potent anticancer drug and highlights its ability in overcoming cisplatin-resistant tumor cells.

To probe the mode of action for 56MESS, multiple *in vitro* and *in vivo* OC models were used. The results showed that 56MESS inhibited proliferation and colony formation. We also found that 56MESS had a potent anticancer effect on oral cancer xenografts. Furthermore, both 56MESS and cisplatin-treated cells caused a G2/M phase arrest. Similar cell cycle arrest is also reported in non-synchronized 56MESS-treated MDCK cells (Garbutcheon-Singh et al. 2013). In addition, we failed to find apoptosis in 56MESS-treated cancer cells, which is consistent with a previous report (Krause-Heuer et al. 2009). Altogether, these data suggest that 56MESS is capable of inducing cell cycle arrest, but not apoptosis.

FACL4, also known as ACSL4, is a long-chain fatty acyl-CoA synthetase. Deregulated FACL4 plays a casual role in the aggressiveness of a variety of malignant tumors (Tang et al. 2018; Sung et al. 2007; Wu et al. 2015). Overexpression of FACL4 is a potential therapeutic target for hepatocellular carcinoma as an independent adverse prognostic parameter (Sun and Xu 2017). Here, we found that FACL4 is upregulated in head and neck cancers. Overexpression of FACL4 fueled cancer cell proliferation. Indeed, FACL4 is implicated in drug resistance in breast cancer cell lines (Orlando et al. 2019). A recent study showed that FACL4 promotes docetaxel resistance in prostate cancer (Jiang et al. 2020). In our study, 56MESS downregulated FACL4 expression, and importantly, FACL4 overexpression counteracted 56MESS-mediated growth inhibition. These data suggest that the action of 56MESS is performed by downregulating FACL4 expression, at least partially.

In sum, our study confirmed that 56MESS is a potent anticancer drug in oral cancer. This activity is partially realized *via* FACL4 downregulation. 56MESS treatment along with FACL4 downregulation may provide a rationale for anticancer therapy.

4. Experimental

4.1. Pt-based compounds

Cisplatin and seven non-classical Pt-based compounds (Fig. 1) including picoplatin, Pt-Acrmatu, 56MESS, phenanthriplatin, pyriplatin, BBR3005, and BBR3571 were synthesized by Prof. H Xiao. The purity of these compounds was tested by ICP-MS.

4.2. Cell culture

Human OC cell lines SCC15, SCC25, CAL27 were purchased from ATCC (Rockville, USA). UM1 was kindly provided by Dr. X. Zhou (University of Illinois at Chicago, USA). HSC3 and CAL33 were kindly provided by J. Silvio Gutkind (NIH, USA). The HSC3, CAL33, and CAL27 cells were cultured in DMEM containing 10% FBS. The SCC15, SCC25 and UM1 cells were grown in DMEM-F12 with 10% FBS. All cells were cultured at 37 °C in a humidified atmosphere containing 5% CO_2.

4.3. Transfection

Cells were transfected with FACL4-overexpression plasmid (EX-T2102-Lv105, GeneCopoeia, China-or control plasmid (EX-EGFP-M02, GeneCopoeia, China) by using Lipofectamine 3000 (Thermo Fisher Scientific, USA) according to the manufacturer's instructions.

4.4. In vitro drug sensitivity assay and cell viability assay

Briefly, 3,000 cells/well were seeded into 96-well plate overnight at 37 °C. The cells were treated with different concentrations of cisplatin and seven non-classical Pt-based compounds for 48 h. The range of drug concentrations was based on published studies and aimed to obtain IC_{50} values. After incubation with CCK-8 reagent (Sigma–Aldrich, USA), the absorbance of the samples was determined with a microplate reader (Genios TECAN, Schweiz) at 450 nm. The assay was conducted in five replicate wells for each sample, and three parallel experiments were performed. For cell viability assay, 3,000 cells/well were seeded in 96-well plates and cells were incubated with 50 μg/ml TMZ for indicated times. Cell viability was determined with CCK-8 kit following the manufacturer's instructions.

4.5. EdU staining assay

The cells were fixed with 4% paraformaldehyde, then permeated with 0.5% TritonX-100. The EdU staining was performed according to the manufacture's procedure (Ribobio, China). Cells were counter-stained with Hoechst 33342 and observed under fluorescent microscopy.

4.6. Colony formation assay

500 cells/well were seeded into 6-well plates. After treated for 10 days, visible colonies were harvested, fixed and stained with crystal violet. Colonies with diameter above 1 mm were counted.

4.7. Flow cytometric analysis

The cells were collected and washed with PBS, and fixed in 70% ethanol at 4 °C overnight. Cell cycle was analyzed by PI staining of nuclei. PI absorbance was determined by fluorescence activated cell sorting on a flow cytometry (Beckman Coulter, Cytoflex, USA). The apoptosis assay was performed using a FITC Annexin V Apoptosis Detection Kit (BD Pharmingen, USA), and analyzed by flow cytometry (Beckman Coulter). Flowojo analysis software was used to calculate the percentage of apoptotic cells.

4.8. Western blot

Cells were incubated with DMSO, CDDP or 56MESS for 48 h. The total protein was extracted using RIPA lysis buffer (Beyotime Biotech, China) containing phosphatase inhibitor (Sigma Aldrich, USA) Protein concentration was measured using a BCA protein assay kit (Beyotime Biotech, China). Equal amounts of the protein samples were loaded and separated by 10% SDS-PAGE and transferred onto PVDF membrane (Millipore, USA). After blocking with 5% bovine serum albumin in TBST buffer (BSA) for 1 h at room temperature, the membranes were incubated at 4 °C overnight with primary antibodies against FACL4 (1:1,000, Abcam, USA), GAPDH (1:1,000, Affinity Biosciences, USA) and β-actin (1:1,000, Cell Signaling Technology, USA). The membranes were washed with TBST buffer and then incubated with the appropriate HRP-conjugated secondary antibodies (1:10,000, Affinity Biosciences-USA) at room temperature for 1h. The bands were visualized with Immun-Star HRP peroxide buffer and Luminol/Enhancer (Bio-Rad, USA), and the luminescence images were analyzed using Alpha Innotech imaging software (San Leandro, USA).

4.9. qRT-PCR

Total RNA was extracted using RNAzol reagent (BD, USA) and reverse transcribed with PrimeScript RT Reagent Kit (Takara, Japan). The following PCR primers were employed:

FACL4, 5'-gctgtaatagacatccctgg-3' (sense) and 5'-cacttaggatttccctggtc-3' (antisense); GAPDH, 5'-catctctgccccctctgctga-3'(sense) and 5'-ggatgaccttgcccacagcct-3' (antisense). PCR assay was performed on triplicate samplesusing SYBR

Premix Ex TaqTM II (Takara, Japan) in a Light Cycler 480 system (Roche, Germany) according to themanufacturer's instructions. The relative expression levels were calculated using the $2^{-\Delta\Delta Ct}$ method after normalized to the control endogenous GAPDH.

4.10. Immunofluorescence

Cells were grown on confocal dishes incubated with 56MESS for 48 h, fixed with 4% paraformaldehyde, permeated and blocked. Then, the cells were incubated with primary antibodies (anti-FACL4, 1:200, Abcam; anti-β-Tubulin 1:200, Cell Signaling Technology) at 4 °C overnight, followed by Fluor594-conjugated goat anti-rabbit IgG(H+L) (1:200, Affinity Biosciences) or Fluor488-conjugated goat anti-mouse IgG(H+L) (1:200, Affinity Biosciences). The cell nuclei were counterstained with DAPI. Images were recorded using a Zeiss LSM 710 laser scanning confocal microscopy (Carl Zeiss, Germany).

4.11. Animal xenografts

All animal experiments were approved by the ethical committees of Sun Yat-sen University and followed the protocol. Four- to six-week-old female BALC/c nude mice were purchased from the Animal Care Unit of Guangdong, China, and maintained in pathogen-free conditions. The mice were randomly divided into three groups (n = 5 per group), and implanted subcutaneously with 5×10^6 cancer cells into flank region of the nude mice. From the xenograft size reached about 100 mm^3 (day 0), the mice received tail vein injection of CDDP (4 mg/kg), 56MESS (4 mg/kg) at their MTD (Moretto et al. 2011), or equivalent volume of DMSO every four days. Tumor growth was routinely observed. Tumor volume (mm^3) was measured using a Vernier caliper and calculated by using the formula: V = (length × $width^2$)/2. Mice were monitored and sacrificed at 24 days after the first treatment.

4.12. Immunohistochemical assay

Paraffin-embedded tumor tissues were cut into 4 μm sections and processed for immunostaining. The sections were incubated overnight at 4 °C with primary antibodies against Ki67 (1:500, Abcam), FACL4 (1:100, Affinity Biosciences) and visualized using 3,3-diaminobenzidine (DAB, Sigma-Aldrich) and counterstained with hematoxylin.

4.13. Mitochondrial membrane potential (MMP) assay

Cells were washed with PBS after harvested. JC-1 mitochondrial membrane potential assay was performed according to the manufacturer's procedure (Beyotime Biotech, China) and observed under a fluorescence microscopy.

4.14. Statistical analysis

All statistical analyses were performed using GraphPad Prism 8.0 (La Jolla, USA). Comparisons between groups were assessed by two-tailed Student's t-test or one-way ANOVA. Difference was considered significant at $P < 0.05$, and designated as follows: $^{*}P < 0.05$; $^{**}P < 0.01$.

Conflicts of interest: None declared.

References

Chopard C, Lenoir C, Rizzato S, Vidal M, Arpalahti J, Gabison L, Albinati A, Garbay C, Kozelka J (2008) Synthetic route to dinuclear Platinum(II) complexes [{trans-PtCl(NH_3)$_2$}$_2$(μ-L)]$^{2+}$(L = aliphatic or heterocyclic diamine) as potential antitumor agents, exploiting the mutual activation of hydroxido ligands and ammonium groups. Inorg Chem 47: 9701–9705.

Chandrashekar DS, Bashel B, Balasubramanya SAH, Creighton CJ, Ponce-Rodriguez I, Chakravarthi BVSK, Varambally S (2017) UALCAN: A portal for facilitating tumor subgroup gene expression and survival analyses. Neoplasia 19: 649–658.

Dasari S, Tchounwou PB (2014) Cisplatin in cancer therapy: Molecular mechanisms of action. Eur J Pharmacol 740: 364–378.

Eckardt JR, Bentsion DL, Lipatov ON, Polyakov IS, MacKintosh FR, Karlin DA, Baker GS, Breitz HB (2009) Phase II study of picoplatin as second-line therapy for patients with small-cell lung cancer. J Clin Oncol 27: 2046–2051.

Garbutcheon-Singh KB, Myers S, Harper BWJ, Ng NS, Dong Q, Xie C, Aldrich-Wright JR (2013) The effects of 56MESS on mitochondrial and cytoskeletal proteins and the cell cycle in MDCK cells. Metallomics 5: 161–167.

Gonzales-Vitale JC, Hayes DM, Cvitkovic E, Sternberg SS (1977) The renal pathology in clinical trials of cis-platinum (II) diamminedichloride. Cancer 39: 1362–1371.

Gregory MT, Park GY, Johnstone TC, Lee YS, Yang W, Lippard SJ (2014) Structural and mechanistic studies of polymerase η bypass of phenanthriplatin DNA damage. Proc Natl Acad Sci USA 111: 9133–9138.

Johnstone TC, Park GY, Lippard SJ (2014) Understanding and improving platinum anticancer drugs--phenanthriplatin. Anticancer Res 34: 471–476.

Jiang X, Guo S, Zhang Y, Zhao Y, Li X, Jia Y, Xu Y, Ma B (2020) LncRNA NEAT1 promotes docetaxel resistance in prostate cancer by regulating ACSL4 via sponging miR-34a-5p and miR-204-5p. Cell Signal 65: 109422.

Krause-Heuer AM, Grünert R, Kühne S, Buczkowska M, Wheate NJ, Le Pevelen DD, Boag LR, Fisher DM, Kasparkova J, Malina J, Bednarski PJ, Brabec V, Aldrich-Wright JR (2009) Studies of the mechanism of action of Platinum(II) complexes with potent cytotoxicity in human cancer cells. J Med Chem 52: 5474–5484.

Monroe JD, Hruska HL, Ruggles HK, Williams KM, Smith ME (2018) Anti-cancer characteristics and ototoxicity of platinum(II) amine complexes with only one leaving ligand. Plos One 13: e192505.

Moretto J, Chauffert B, Ghiringhelli F, Aldrich-Wright JR, Bouyer F (2011) Discrepancy between in vitro and in vivo antitumor effect of a new platinum(II) metallointercalator. Invest New Drugs 29: 1164–1176.

Orlando UD, Castillo AF, Medrano MAR, Solano AR, Maloberti PM, Podesta EJ (2019) Acyl-CoA synthetase-4 is implicated in drug resistance in breast cancer cell lines involving the regulation of energy-dependent transporter expression. Biochem Pharmacol 159: 52–63.

Park GY, Wilson JJ, Song Y, Lippard SJ (2012) Phenanthriplatin, a monofunctional DNA-binding platinum anticancer drug candidate with unusual potency and cellular activity profile. Proc Natl Acad Sci USA 109: 11987–11992.

Siegel RL, Miller KD, Jemal A (2020) Cancer statistics, 2020. CA Cancer J Clin 70: 7–30

Suryadi J, Bierbach U (2012) DNA Metalating-Intercalating hybrid agents for the treatment of chemoresistant cancers. Chemistry 18: 12926–12934.

Sung YK, Park MK, Hong SH, Hwang SY, Kwack MH, Kim JC, Kim MK (2007) Regulation of cell growth by fatty acid-CoA ligase 4 in human hepatocellular carcinoma cells. Exp Mol Med 39: 477–482.

Sun XJ, Xu GL (2017) Overexpression of Acyl-CoA ligase 4 (ACSL4) in patients with hepatocellular carcinoma and its prognosis. Med Sci Monit 23: 4343–4350.

Tang C, Parham C, Shocron E, McMahon G, Patel N (2011) Picoplatin overcomes resistance to cell toxicity in small-cell lung cancer cells previously treated with cisplatin and carboplatin. Cancer Chemother Pharm 67: 1389–1400.

Tang Y, Zhou J, Hooi SC, Jiang Y, Lu G (2018) Fatty acid activation in carcinogenesis and cancer development: Essential roles of long-chain acyl-CoA synthetases. Oncol Lett 16: 1390–1396.

Wang S, Higgins VJ, Aldrich-Wright JR, Wu MJ (2012) Identification of the molecular mechanisms underlying the cytotoxic action of a potent platinum metallointercalator. J Chem Biol 5: 51–61.

Wang X, Martindale JL, Holbrook NJ (2000) Requirement for ERK activation in cisplatin-induced apoptosis. J Biol Chem 275: 39435–39443.

Wu X, Deng F, Li Y, Daniels G, Du X, Ren Q, Wang J, Wang LH, Yang Y, Zhang V, Zhang D, Ye F, Melamed J, Monaco ME, Lee P (2015) ACSL4 promotes prostate cancer growth, invasion and hormonal resistance. Oncotarget 6: 44849–44863.

Yu Z, Zhong L, Ji T, Zhang P, Chen W, Zhang C (2010) MicroRNAs contribute to the chemoresistance of cisplatin in tongue squamous cell carcinoma lines. Oral Oncol 46: 317–322.

Zhu G, Myint M, Ang WH, Song L, Lippard SJ (2012) Monofunctional platinum-DNA adducts are strong inhibitors of transcription and substrates for nucleotide excision repair in live mammalian cells. Cancer Res 72: 790–800.

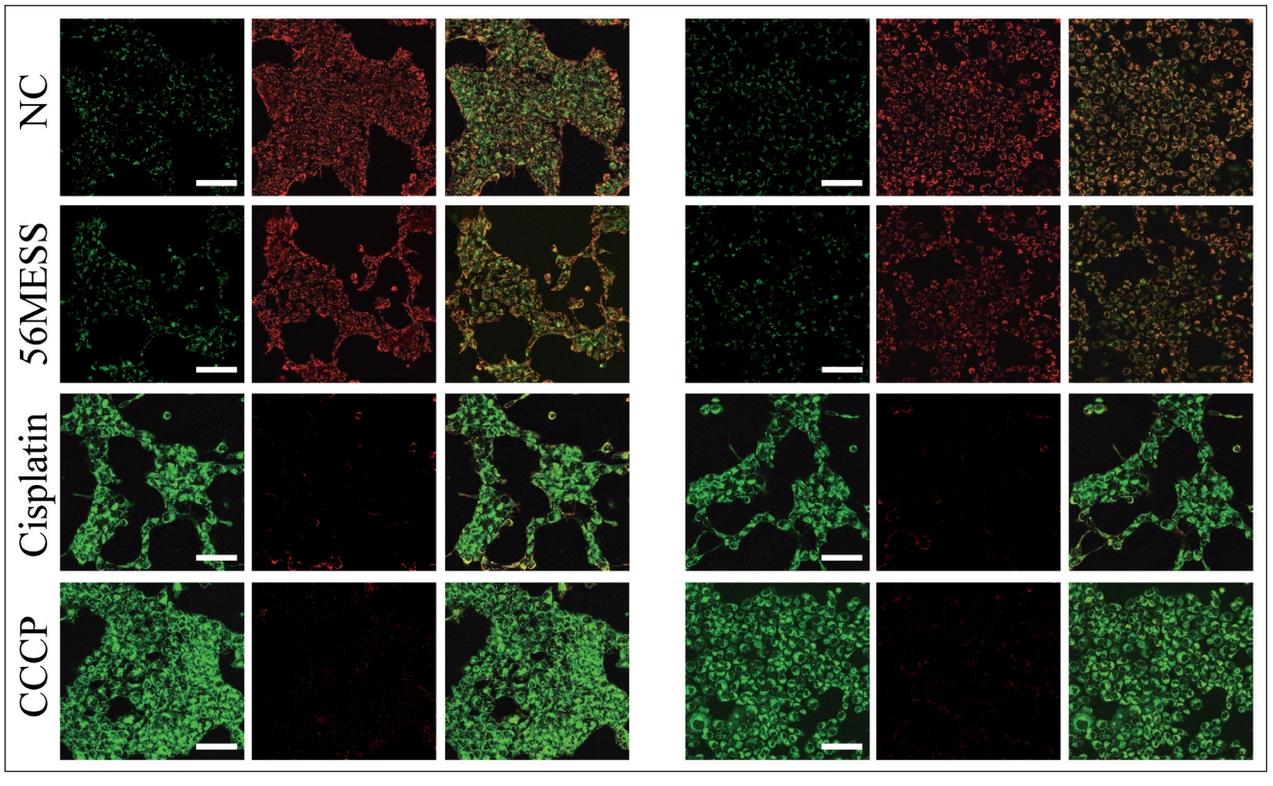

Supplementary Fig. 1: No change of mitochondrial membrane potential (MMP) in 56MESS treated CAL33 and SCC25 cells. Analysis of MMP in cells after 56MESS or cisplatin treatment for 48 h. The green portion increasing compared to the red part indicates MMP hyperpolarization, and accordingly, causes cell apoptosis. Carbonylcyanide3-chlorophenylhydrazone (CCCP, 5 mM) treatment is used as positive control. NC: negative control (DMSO treatment). Scale bar: 100 μM.

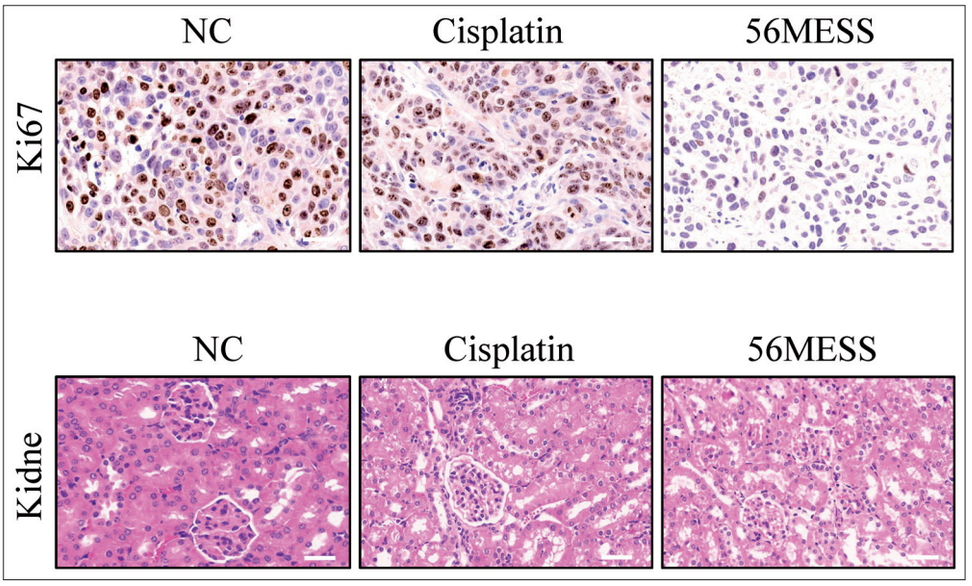

Supplementary Fig. 2: A. Ki67 immunostaining in the treated xenografts. B. H&E staining of the kidney. Scale bar: 100 μM.

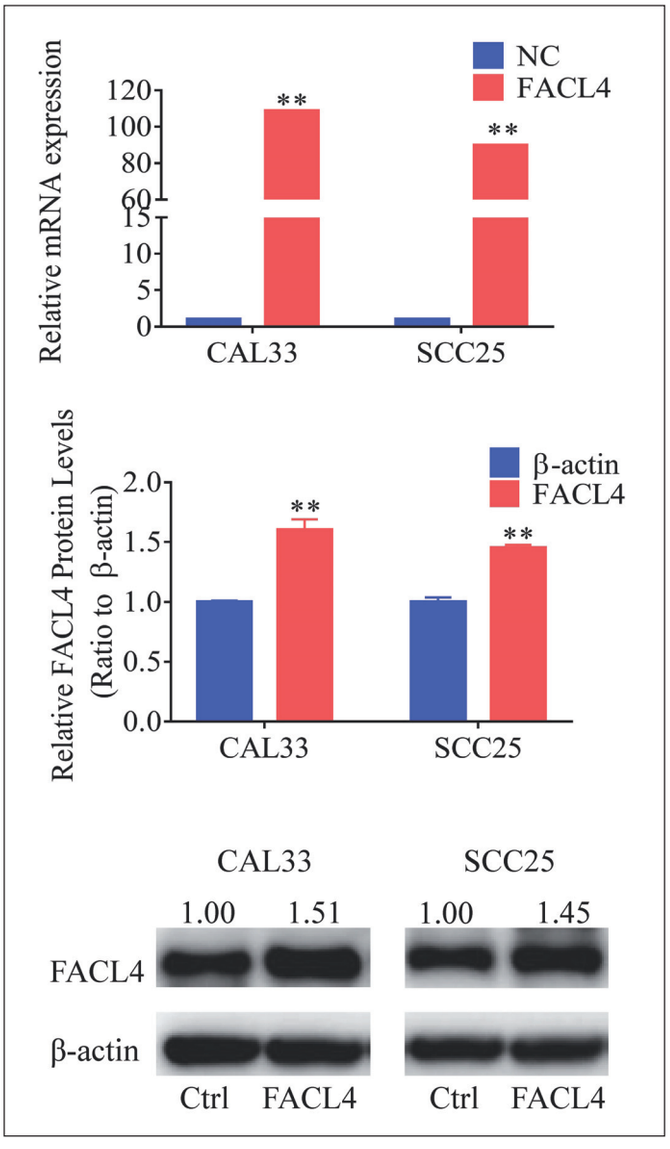

Supplementary Fig. 3: The relative expression level of FACL4 mRNA and protein in cancer cells after transfected with FACL4-overexpression plasmid. **P < 0. 01.